Phase transition to synchronization in generalized Kuramoto model with low-pass filter

Wei Zou,[1,*] Meng Zhan,[2] and Jürgen Kurths[3,4,5]

[1]*School of Mathematical Sciences, South China Normal University, Guangzhou 510631, China*

[2]*State Key Laboratory of Advanced Electromagnetic Engineering and Technology, School of Electrical and Electronic Engineering, Huazhong University of Science and Technology, Wuhan 430074, China*

[3]*Potsdam Institute for Climate Impact Research, Telegraphenberg, Potsdam D-14415, Germany*

[4]*Institute of Physics, Humboldt University Berlin, Berlin D-12489, Germany*

[5]*Saratov State University, Saratov 4410012, Russia*

(Received 24 May 2019; published 15 July 2019)

A second-order continuous synchronization has been well documented for the classic Kuramoto model. Here we generalize the classic Kuramoto model by incorporating a low-pass filter (LPF) in the coupling, which serves as a simple form of indirect coupling through a common external dynamic environment. We uncover that a first-order explosive synchronization turns out to be a very generic phenomenon in this generalized Kuramoto model with LPF. We establish theoretical results by providing a rigorous analytical treatment, which is validated by conducting extensive numerical simulations. Our study provides a new root for the emergence of first-order explosive synchronization, which could substantially deepen the understanding of the underlying mechanism of a first-order phase transition towards synchronization in coupled dynamical networks.

DOI: 10.1103/PhysRevE.100.012209

I. INTRODUCTION

Spontaneous synchronization is a ubiquitous emergent behavior of a population of interacting elements in many contexts of physics, biology, and even social systems [1–3]. One prototype for studying synchronization was introduced by Kuramoto in 1975 [4]. For the classic Kuramoto model, it was exclusively reported that the process from incoherence to synchrony typically takes place via a second-order continuous phase transition [4–7], which has been experimentally identified in coupled chemical oscillators [8]. Later, a first-order discontinuous transition to synchronization was recognized if the coupling has a time delay [9–11] or the natural frequencies are bimodally distributed [12–14]. In particular, a first-order phase transition towards synchronization was further discovered in scale-free networks of coupled Kuramoto oscillators [15], where this phenomenon is termed *explosive* synchronization. Since then, an ever-increasing theoretical interest has been witnessed in uncovering the roots for the onset of explosive synchronization [16–21].

Hitherto, advances of explosive synchronization in the Kuramoto model have been made for the case of direct coupling via the differences of their phases [15–22]. However, in a wide variety of realistic systems, the interaction between units occurs indirectly through an external agency or medium. Typical examples include synthetic gene-regulation networks based on cell-to-cell communication [23–26], catalytic microparticles in a Belousov-Zhabotinsky reaction [27–29], suspensions of yeast in nutrient solutions [30], semiconductor lasers optically linked by a central hub [31], degrade-and-fire oscillators coupled through a common activator [32], etc. In this work, we generalize the classic Kuramoto model by incorporating a conventional low-pass filter (LPF) into the coupling, which provides a bridge linking the direct coupling to the indirect one. The coupling with LPF serves as a minimal form of indirect interaction through a common external environment, which is synthesized by the contributions of all units analogous to dynamical quorum sensing [23–35].

In many real-world systems, signals are generally inevitable to be distorted during their transmissions due to the diverse physical limitations of channels [36–38]. Consequently, it is of practical importance to take into account the effects of communication channels on emergent dynamics of coupled systems. The LPF serves as a basic protocol to capture the frequency-selective property of the communication channels of physical systems [39–41]. However, the phase transition to synchronization still remains unclear in the presence of LPF in coupled dynamical networks. A significant task here is to systematically study the phase transition towards synchronization in an indirectly coupled Kuramoto model with LPF, which will introduce a deeper insight into the roots of the first-order explosive synchronization.

In this work, we exclusively establish both the second- and the first-order phase transitions to synchronization in the generalized Kuramoto model with LPF. We report that the second-order continuous synchronization can transit to the first-order explosive one, which is consolidated by performing rigorous theoretical analyses, and then numerically confirmed by carrying out a series of simulations. The generalized Kuramoto model with LPF is the simplest exactly solvable case for indirectly coupled dynamical networks through a common external medium, which undergoes two distinct kinds of phase transitions towards synchronization depending on the cutoff frequency of the filter. Our study serves as a promising recipe in unveiling the rich behaviors of phase transitions in indirectly coupled dynamical networks.

*weizou83@gmail.com

II. KURAMOTO MODEL WITH LPF

Let us begin with an ensemble of N Stuart-Landau limit-cycle oscillators coupled diffusively via a common external medium,

$$\dot{Z}_j = (1 + iw_j - |Z_j|^2)Z_j + K(\mu - Z_j), \tag{1}$$

$$\alpha\dot{\mu} = -\mu + \frac{1}{N}\sum_{k=1}^{N} Z_k, \tag{2}$$

where $j = 1, \ldots, N$. w_j is the intrinsic frequency of the jth oscillator distributed according to a prescribed density $g(w)$. K accounts for the overall coupling strength. The external medium μ described by Eq. (2) stands for a conventional LPF with a time constant $\alpha > 0$ to attenuate the mean-field signal, which mediates the coupling between oscillators qualitatively resembling the interaction way of dynamical quorum sensing [23–31]. For weak coupling of strength or the strong attractiveness of a limit-cycle orbit, the dynamics of an individual unit can be well captured only by its phase variable, where the amplitude of the limit cycle remains unaffected. By rewriting $Z_j = e^{i\theta_j}$ and $\mu = \rho e^{i\phi}$, Eqs. (1) and (2) are reduced to the phase-only model:

$$\dot{\theta}_j = w_j + K\rho\sin(\phi - \theta_j), \tag{3}$$

$$\alpha\dot{\mu} = -\mu + z. \tag{4}$$

Here $z = re^{i\psi} = \frac{1}{N}\sum_{k=1}^{N} e^{i\theta_k}$ defines the Kuramoto order parameter, where r ($0 \leqslant r \leqslant 1$) and ψ quantify the degree of coherence and the average phase of the oscillator community, respectively.

If $\alpha = 0$, Eqs. (3) and (4) degenerate to the classic Kuramoto model with direct coupling [4–6]. It has been well documented that, when $g(w)$ is assumed to be unimodal and even about a mean frequency w_0, the stationary value of r as a function of the coupling strength K shows a typical second-order phase transition from incoherence $r = 0$ to coherence $r > 0$ with a critical coupling strength $K_c = 2/[\pi g(w_0)]$ [5]. In the setting of $\alpha > 0$, Eqs. (3) and (4) generalize the classic Kuramoto model by incorporating a LPF in the coupling. We will reveal that the phase synchronization can also proceed discontinuously and irreversibly via a first-order fashion for $\alpha > 0$.

With shifting to a frame rotating with frequency w_0, Eq. (4) is then replaced by

$$\alpha\dot{\mu} = -(1 + i\alpha w_0)\mu + z, \tag{5}$$

where Eq. (3) remains unchanged, but w_j is now extracted from a new density function $\widetilde{g}(w)$ with zero mean value and the same profile to $g(w)$, i.e., $\widetilde{g}(w) = g(w + w_0)$.

III. STABILITY ANALYSIS OF INCOHERENCE

In the thermodynamic limit of $N \to \infty$, the dynamics of phases θ_j in Eq. (3) can be described by the time-dependent density function $F(\theta, w, t)$ [5], where $F(\theta, w, t)\,d\theta\,dw$ represents the ratio of oscillators with phases between θ and $\theta + d\theta$ and natural frequencies between w and $w + dw$ at time t with the normalization condition

$$\int_0^{2\pi} F(\theta, w, t)\,d\theta = 1. \tag{6}$$

$F(\theta, w, t)$ obeys the continuity equation

$$\frac{\partial F}{\partial t} + \frac{\partial}{\partial\theta}(Fv) = 0, \tag{7}$$

where the phase velocity $v = \dot{\theta}$ is given by

$$v = w + K\rho\sin(\phi - \theta) = w + \frac{K}{2i}(\mu e^{-i\theta} - \mu^* e^{i\theta}). \tag{8}$$

In the setting of $N \to \infty$, the Kuramoto order parameter z has the integral form

$$z = re^{i\psi} = \int_{-\infty}^{+\infty}\int_0^{2\pi} e^{i\theta}\widetilde{g}(w)F(\theta, w, t)\,d\theta\,dw. \tag{9}$$

The density function $F(\theta, w, t)$ is 2π-periodicity in θ, which can be expressed in the form of the Fourier expansion

$$F(\theta, w, t) = \frac{1}{2\pi}\sum_{n=-\infty}^{+\infty} z_n(t, w)e^{-in\theta} \tag{10}$$

with the nth Fourier coefficient

$$z_n(t, w) = \int_0^{2\pi} e^{in\theta}F(\theta, w, t)\,d\theta, \quad n = 0, 1, 2, \ldots, \tag{11}$$

where $z_0(t, w) = 1$ and $z_{-n}(t, w) = z_n^*(t, w)$. The Kuramoto parameter $z(t)$ is then given by

$$z(t) = \int_{-\infty}^{+\infty} z_1(t, w)\widetilde{g}(w)\,dw. \tag{12}$$

The evolutions of $z_n(t, w)$ satisfy the differential equations

$$\frac{dz_n}{dt} = niwz_n + \frac{nK}{2}(\mu z_{n-1} - \mu^* z_{n+1}) \text{ for } n \geqslant 1. \tag{13}$$

Equations (5), (12), and (13) constitute a closed description for the macroscopic dynamics of the full system. The incoherent state corresponds to $\mu = 0$ and $z_n = 0$ for $n = 1, 2, \ldots$, for which $F(\theta, w, t) = 1/2\pi$ and $r = 0$. By linearizing Eqs. (5), (12), and (13) around the origin, we get a set of the following linear equations:

$$\frac{d\delta z_1}{dt} = iw\delta z_1 + \frac{K}{2}\delta\mu, \tag{14}$$

$$\frac{d\delta z_n}{dt} = inw\delta z_n, \text{ for } n > 1, \tag{15}$$

$$\alpha\frac{d\delta\mu}{dt} = -(1 + i\alpha w_0)\delta\mu + \delta z, \tag{16}$$

where

$$\delta z = \int_{-\infty}^{+\infty} \delta z_1(t, w)\widetilde{g}(w)\,dw. \tag{17}$$

From Eq. (15), all higher Fourier harmonics δz_n ($n > 1$) are neutrally stable. Thus, only δz_1 is needed to be considered for the stability of the incoherence. Equations (14) and (16) can be rewritten in the compact form

$$\begin{pmatrix}\dot{\delta z_1}\\ \dot{\delta\mu}\end{pmatrix} = \begin{pmatrix} iw, \frac{K}{2}\\ \frac{1}{\alpha}\widehat{P}, -\frac{1+i\alpha w_0}{\alpha}\end{pmatrix}\begin{pmatrix}\delta z_1\\ \delta\mu\end{pmatrix} = \widehat{T}\begin{pmatrix}\delta z_1\\ \delta\mu\end{pmatrix}, \tag{18}$$

where $\widehat{P}$ denotes a linear operator defined as

$$\widehat{P}q(w) = \int_{-\infty}^{+\infty} q(w)\widetilde{g}(w)\,dw = (q(w), P_0). \tag{19}$$

Assume that the linear operator $\widehat{T}$ has the eigenvalue a:

$$\widehat{T}\begin{pmatrix}\delta z_1\\ \delta\mu\end{pmatrix} = a\begin{pmatrix}\delta z_1\\ \delta\mu\end{pmatrix}. \tag{20}$$

Substituting the form of $\widehat{T}$ into Eq. (20) leads to

$$\frac{K}{2}(a - iw)^{-1}\widehat{P}\delta z_1 = (1 + \alpha a + i\alpha w_0)\delta z_1. \tag{21}$$

Applying the inner product with P_0 for both sides of Eq. (21), we obtain

$$1 + \alpha a + i\alpha w_0 = \frac{K}{2}\int_{-\infty}^{+\infty} \frac{\widetilde{g}(w)}{a - iw}\,dw, \quad a \neq iw. \tag{22}$$

The solution of Eq. (22) gives the discrete spectrum, where $a = iw$ constitutes the continuous spectrum [5]. The critical coupling K_c at which the incoherent state loses its stability while increasing K beyond K_c corresponds to a solution of Eq. (22) with $\mathrm{Re}a \to 0^+$. Let $a = \lambda - i\beta$ and $\lambda \to 0^+$ in Eq. (22), and separate the real and imaginary parts, then K_c is determined by

$$K_c = \frac{2}{\pi\tilde{g}(\beta)}, \tag{23}$$

where β satisfies

$$\alpha(w_0 - \beta)\pi\tilde{g}(\beta) = P.V.\int_{-\infty}^{+\infty} \frac{\tilde{g}(w)}{\beta + w}\,dw. \tag{24}$$

To arrive at Eqs. (23) and (24), the Sokhotski-Plemelj formula is used [42], where *P.V.* denotes the Cauchy principle-value integration. For $\alpha \to 0$, $\beta = 0$ solves the Eq. (24), thus $K_c = \frac{2}{\pi\tilde{g}(0)} = \frac{2}{\pi g(w_0)}$ for $\alpha = 0$, which well recovers the same result of the classic Kuramoto model [4–6].

For a general frequency distribution $\widetilde{g}(w)$, the critical coupling strength K_c in Eqs. (23) and (24) cannot be derived explicitly. However, for a Lorentzian distribution $g(w) = \Delta/\pi[(w - w_0)^2 + \Delta^2]$, K_c can be obtained analytically. First, the integral in the right side of Eq. (22) can be treated as

$$\begin{aligned}\int_{-\infty}^{+\infty} \frac{\widetilde{g}(w)}{a - iw}\,dw &= \int_{-\infty}^{+\infty} dw \int_0^{+\infty} e^{-(a-iw)s}\widetilde{g}(w)\,ds\\ &= \int_0^{+\infty} ds e^{-as}\int_{-\infty}^{+\infty} e^{iws}\widetilde{g}(w)\,dw\\ &\equiv \int_0^{+\infty} e^{-as}G(s)\,ds,\end{aligned} \tag{25}$$

where

$$G(s) = \int_{-\infty}^{+\infty} e^{iws}\widetilde{g}(w)\,dw \tag{26}$$

is the characteristic function by performing the Fourier transformation of the density function $\widetilde{g}(w)$. For a Lorentzian distribution $\widetilde{g}(w) = \Delta/\pi(w^2 + \Delta^2)$, its characteristic function is explicitly given by

$$G(s) = e^{-\Delta|s|}. \tag{27}$$

Plugging Eq. (27) into Eq. (25) yields

$$\int_{-\infty}^{+\infty} \frac{\widetilde{g}(w)}{a - iw}\,dw = \frac{1}{a + \Delta}. \tag{28}$$

Thus, the discrete spectrum in Eq. (22) is decided by

$$(1 + \alpha a + i\alpha w_0)(a + \Delta) = \frac{K}{2}. \tag{29}$$

By letting $a = \lambda - i\beta$ and $\lambda \to 0^+$ in Eq. (29), and separating the real and imaginary parts, K_c is solved out as

$$K_c = 2\Delta + \frac{2\Delta\alpha^2 w_0^2}{(1 + \Delta\alpha)^2}. \tag{30}$$

IV. SOLUTION OF COHERENCE

For the Lorentzian distribution $g(w)$, the evolution of the Kuramoto order paramter z can be explicitly worked out with the Ott-Antonsen *ansatz* [43,44]. First, by expanding $F(\theta, w, t)$ in a Fourier series

$$F(\theta, w, t) = \frac{1}{2\pi}\left\{1 + \sum_{n=1}^{\infty}[a^n(w, t)e^{in\theta} + a^n(w, t)^* e^{-in\theta}]\right\}, \tag{31}$$

then substituting the above form of $F(\theta, w, t)$ back into the continuity Eq. (7) leads to

$$\frac{\partial a}{\partial t} + iwa + \frac{K}{2}(\mu a^2 - \mu^*) = 0. \tag{32}$$

The Kuramoto order parameter z is expressed as

$$\begin{aligned}z = re^{i\psi} &= \int_{-\infty}^{+\infty}\int_0^{2\pi} e^{i\theta}g(w)F(\theta, w, t)\,d\theta\,dw\\ &= \int_{-\infty}^{+\infty} a^*(w, t)g(w)\,dw.\end{aligned} \tag{33}$$

For a Lorentzian distribution $g(w) = \Delta/\pi[(w - w_0)^2 + \Delta^2]$, we have $\int_{-\infty}^{+\infty} a^*(w, t)g(w)\,dw = a^*(w_0 - i\Delta, t)$. Thus, the evolution of z is

$$\dot{z} = -\Delta z + iw_0 z + \frac{K}{2}(\mu - \mu^* z^2). \tag{34}$$

Equation (34) together with Eq. (4) form a closed ODE system. By introducing the polar coordinates of $z = re^{i\psi}$ and $\mu = \rho e^{i\phi}$, and setting $\dot{r} = \dot{\rho} = 0$ and $\dot{\psi} = \dot{\phi} = \Omega$, a stationary behavior of $r = |z| > 0$ for the coherent state is given by

$$r = \sqrt{1 - \frac{2\Delta(1 + \Delta^2\alpha^2\Omega^2)}{K}}, \tag{35}$$

where the fixed angular velocity Ω is implicitly determined by

$$A\Omega^3 + B\Omega^2 + C\Omega + D = 0, \tag{36}$$

where $A = (\Delta\alpha - 1)\Delta^2\alpha^2$, $B = w_0\Delta\alpha^2$, $C = \Delta\alpha - 1 - \alpha K$, and $D = w_0/\Delta$.

If $\Delta\alpha = 1$, the expression for Ω determined by Eq. (36) is explicitly derived as

$$\Omega_{\mp} = \frac{K \mp \sqrt{K^2 - 4w_0^2}}{2w_0}. \tag{37}$$

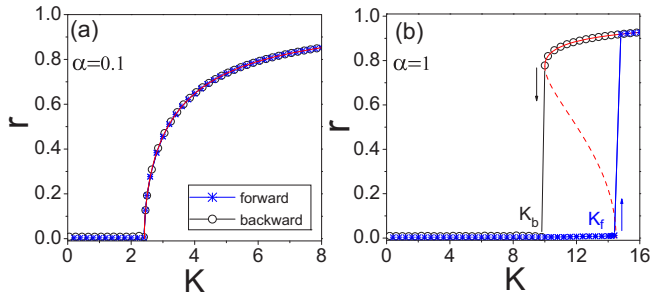

FIG. 1. Synchronization diagrams by plotting r as a function of K for Eqs. (3) and (4) with a Lorentzian frequency distribution $g(w) = \Delta/\pi[(w - w_0)^2 + \Delta^2]$. (a), (b) The plots of r vs K for $\alpha = 0.1$ and $\alpha = 1.0$. Blue line with stars and black line with circles represent numerical simulations of the forward and back synchronization transitions, respectively. Solid (dashed) red line denotes the theoretical prediction for the stable (unstable) branch r_+ (r_-) of $r > 0$. $w_0 = 5$ and $\Delta = 1$ are fixed. $N = 10\,000$ is used in the simulations.

Corresponding to the above $\Omega_\mp$, the exact result of r is further obtained as

$$r_\pm = \frac{\sqrt{w_0^2 - \Delta K \pm \Delta\sqrt{K^2 - 4w_0^2}}}{w_0}, \tag{38}$$

respectively. For $w_0 > 2\Delta$, $r_\pm$ are born via a saddle node bifurcation at $K = 2w_0$, which persist within a pronounced coupling interval of $2w_0 < K < 2\Delta + \frac{w_0^2}{2\Delta}$. Only r_+ survives if $K \geqslant 2\Delta + \frac{w_0^2}{2\Delta}$. In contrast, for $w_0 \leqslant 2\Delta$, only r_+ appears once $K \geqslant K_c = 2\Delta + \frac{w_0^2}{2\Delta}$. r_+ and r_- correspond to a stable and an unstable branch of synchronous states, respectively. Thus, a bistable region with an associated hysteretic loop in r appears for $2w_0 < K < 2\Delta + \frac{w_0^2}{2\Delta}$ if $w_0 > 2\Delta$. For $\Delta\alpha \neq 1$, the analytical expressions for both Ω and r are difficult to be explicitly expressed; however, by numerically solving Eqs. (35) and (36), the solution structure of r is found to be quite similar to those for $\Delta\alpha = 1$.

Our above analytical analysis implies that the transition from a second-order continuous to a first-order explosive synchronization can be induced by the LPF coupling with $\alpha > 0$. To clearly validate this assertion, Figs. 1(a) and 1(b) depict the dependence of r on K for $\alpha = 0.1$ and $\alpha = 1$, where $g(w)$ is assumed to be a Lorentzian distribution. In our simulations [45], two sets of numerical trials, termed *forward* and *backward* continuations, are adopted to monitor the stationary value of r as adiabatically increasing or decreasing K, which are indicated by the blue line with stars and the black line with circles in Fig. 1, respectively. The other parameters $w_0 = 5$, $\Delta = 1$, and $N = 10\,000$ are fixed.

A typical second-order phase transition from the incoherence to synchronization is observed in Fig. 1(a) with $\alpha = 0.1$. In the synchronization diagrams, the value of r as a function of K for the forward and the backward continuations shows a perfect match, where the incoherent state with $r = 0$ is destabilized via a supercritical Hopf bifurcation at $K = K_c$. The red line denoting the theoretical prediction of $r > 0$ from Eqs. (35) and (36) agrees very well with the numerical results of r.

Strikingly, for $\alpha = 1$ in Fig. 1(b), the diagrams of the phase transition to synchronization for the backward and the forward continuations are found to be rather different. In the case of the forward continuation, the order parameter r first remains near zero ($r \simeq 0$), implying the incoherence of the coupled system. Then r jumps suddenly to $r = r_+(K_f) \simeq 1$ at $K_f = K_c = 2\Delta + \frac{w_0^2}{2\Delta} = 14.5$, where the incoherent state loses its stability via a subcritical Hopf bifurcation. For the backward continuation, the coupled system experiences a sharp transition from the synchronized state with $r = r_+(K_b) \simeq 1$ to the incoherence with $r \simeq 0$ at the saddle node bifurcation point of $K = K_b = 2w_0 = 10 < K_f$. Either increasing or decreasing progressively the value of K in the forward or backward direction, the stationary behavior of $r > 0$ is well predicted by r_+ in Eq. (38) delimited by the solid red line, where the unstable branch r_- plotted by the dashed red line is responsible for the emergence of a hysteretic loop in r associated to the first-order explosive synchronization.

The stability of the incoherence is lost completely progressively increasing K from zero to $K = K_f$, which corresponds to the threshold condition to get the phase-synchronized state starting from the incoherence. Thus, one can infer that $K_f = K_c$, where K_c is explicitly given by Eq. (30). The backward critical coupling strength K_b, at which the stability of coherent state is totally destroyed as gradually decreasing K from a sufficiently large value, is implicitly decided by Eq. (36). From Eq. (36), K can be extracted as

$$K = \frac{A\Omega^3 + B\Omega^2 + (\Delta\alpha - 1)\Omega + D}{\alpha\Omega}. \tag{39}$$

At the critical backward transition point $K = K_b$, a saddle node bifurcation emerges, and thus the constraint $dK/d\Omega = 0$ is satisfied, which leads to

$$2A\Omega^3 + B\Omega^2 - D = 0. \tag{40}$$

K_b can be obtained by first solving Ω from Eq. (40) and then inserting the value back into Eq. (39).

Figure 2(a) displays the dependences of K_f and K_b on α, which provides a more exhaustive description of the transition from the second-order to the first-order synchronization. The above theoretical predictions of K_f and K_b are delineated by the black and red lines, which are in good agreement with the direct simulation results of the forward and backward transition points, denoted by the black circles and blue stars, respectively. The first-order phase transition with a hysteretic loop is observed only if $\alpha > \alpha_c = 0.51$, otherwise the phase transition is of the second order. Figure 2(b) further portrays α_c as a function of w_0, where α_c is well predicted from the relation

$$w_0 = \frac{(\Delta\alpha + 1)^{3/2}}{\alpha(3\Delta\alpha - 1)^{1/2}}. \tag{41}$$

The relation of w_0 on α_c in Eq. (41) is derived based on the observation that at the critical point α_c the Hopf bifurcation merges with the saddle node bifurcation in the limit of $r \to 0$. For the synchronized state $r > 0$, the function of Ω on r is $\Omega = w_0/(\Delta + \frac{1+r^2}{1-r^2}\Delta^2\alpha)$. Inserting

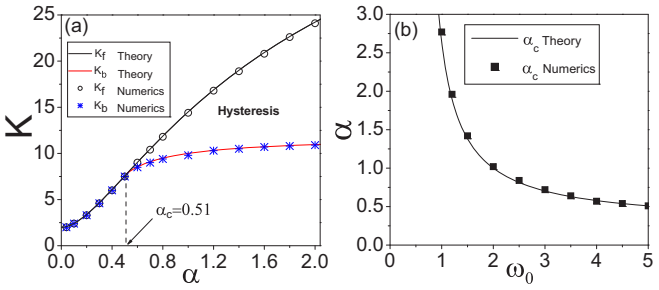

FIG. 2. Characterization of the emergence of a hysteresis in Eqs. (3) and (4) for the Lorentzian frequency distribution $g(w)$ with $\Delta = 1$. (a) K_f and K_b vs α for $w_0 = 5$. The black and red curves correspond to the theoretical predictions of K_f and K_b, which perfectly coincide with the numerical results marked by the blue stars and open circles, respectively. The hysteresis exists only for $\alpha > \alpha_c = 0.51$. (b) The dependence of α_c on w_0. The black square marks the numerical result of α_c, which is well located on the black curve plotted from the relation of Eq. (41).

$\Omega = w_0/(\Delta + \Delta^2\alpha)$ for $r \to 0$ to $dK/d\Omega = 0$ leads to Eq. (41). It is evident from Eq. (41) that the occurrence of the first-order explosive synchronization critically depends on the values of both α and w_0. The onset of a sharp transition with a hysteresis towards synchronization is possible if both $\alpha > \alpha_{\min} = 1/(3\Delta)$ and $w_0 > w_{\min} = \Delta/\sqrt{3}$ hold simultaneously; otherwise only the first-order phase transition can be established.

The LPF coupling can induce the first-order explosive synchronization transition in the generalized Kuramoto model for various other configurations of frequency distributions. We have numerically computed the forward and backward

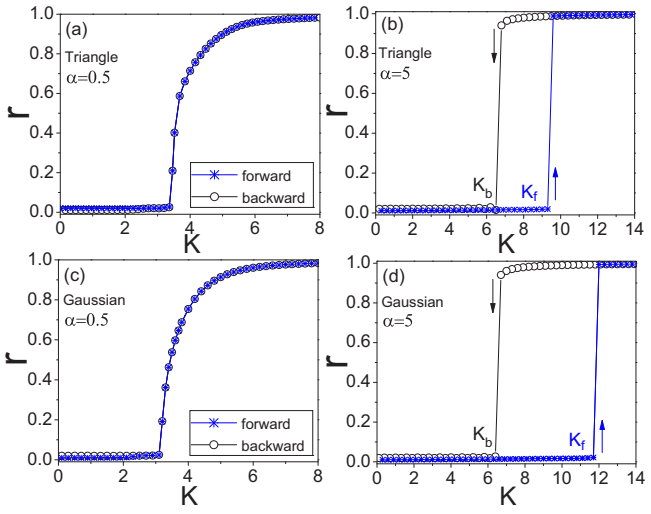

FIG. 3. Synchronization diagrams by plotting r as a function of K for triangle frequency distribution (a), (b) and Gaussian frequency distribution (c), (d). $\alpha = 0.5$ for panels (a) and (c), and $\alpha = 5$ for panels (b) and (d). The triangle distribution is prescribed by $g(w) = (\pi\Delta - |w - w_0|)/\pi^2\Delta^2$ for $|w - w_0| < \pi\Delta$, and 0 otherwise; and the Gaussian distribution by $g(w) = (1/\pi\Delta)\exp(-(w - w_0)^2/\pi\Delta^2)$. $w_0 = 3$, $\Delta = 1$, and $N = 2000$ are used in all simulations.

synchronization diagrams for a triangle frequency distribution [Figs. 3(a) and 3(b)] and a Gaussian frequency distribution [Figs. 3(c) and 3(d)], respectively. For both distributions, a typical second-order phase transition is observed for $\alpha = 0.5$ in Figs. 3(a) and 3(c); however, the two synchronization diagrams in Figs. 3(b) and 3(d) display the phase transition of the first order with a strong hysteresis for $\alpha = 5$. From the four panels of Fig. 3, we notice that $K_f = K_c$ differs for the different frequency configurations of $g(w)$ and depends on the value of α, which is well predicted by Eqs. (23) and (24). The results in Fig. 3 quite resemble those of Fig. 1, corroborating the scalability of the LPF in sustaining the evolution from the second-order to the first-order phase transition towards synchronization.

V. CONCLUSION AND DISCUSSIONS

To conclude, we have reported the transition from the second-order continuous to the first-order explosive synchronization in the generalized Kuramoto model with LPF. As far as the units interact with each other via a shared external medium of the LPF form, we have uncovered that the first-order explosive synchronization turns out to be a very generic phenomenon. The underlying physical mechanism is due to that the inertial feature of LPF effectively introduces a phase-lag (time-delayed) effect between the interaction of coupled systems. However, the coupling with LPF has its own great merits in inducing the first-order explosive synchronization, as is described by a set of linear ordinary differential equations involving only a finite of inherent degrees of freedom, which endows the dynamics of coupled systems to be analytically treated in the theory.

Our proposed LPF coupling can be regarded as a minimal form of indirect interaction via a common external information pool, which gives rise to an equivalent role of coupling to that of dynamical quorum sensing omnipresent in coupled biological and chemical systems. On the other hand, the Kuramoto model is widely recognized as a generic prototype to reveal the general mechanisms of synchronous behaviors observed in diverse natural systems. Thus, our theoretical findings of the generalized Kuramoto model with LPF are supposed to be of widespread practical applications in indirectly coupled systems, where the communications between units are realized via a common external dynamic medium such as in populations of synthetic bacteria and Belousov-Zhabotinsky reactions. By introducing LPF in the Kuramoto model, we have made an important step to systematically study the phase transitions towards synchronization in coupled dynamical networks with LPF, which would initiate numerous further investigations of collective dynamics in indirectly coupled nonlinear networks. Finally, we believe that the transition from the second-order continuous to the first-order explosive synchronization induced by LPF can be evidenced in pertinent experiments such as in coupled electrochemical reactions.

ACKNOWLEDGMENTS

W.Z. would like to acknowledge valuable discussions with István Z. Kiss and J. Luis Ocampo-Espindola through email

exchanges. W.Z. acknowledges support from Research Starting grants from South China Normal University (8S0340) and a project supported by Guangdong Province Universities and Colleges Pearl River Scholar Funded Scheme (2018). M.Z. acknowledges support from the National Natural Science Foundation of China under Grant No. 11475253 and the International (Regional) Cooperation and Exchange Program of the National Natural Science Foundation of China (Research on Inter-organizational Cooperation, NSFC-DFG; Grant No. 11861131011).

[1] S. H. Strogatz, *Sync: The Emerging Science of Spontaneous Order* (Hyperion, New York, 2003).
[2] A. Pikovsky, M. Rosenblum, and J. Kurths, *Synchronization: A Universal Concept in Nonlinear Sciences* (Cambridge University Press, Cambridge, 2001).
[3] Y. Kuramoto, *Chemical Oscillations, Waves, and Turbulence* (Springer, Berlin, 1984).
[4] Y. Kuramoto, in *International Symposium on Mathematical Problems in Theoretical Physics*, edited by H. Araki, Lecture Notes in Physics No. 30 (Springer, New York, 1975), p. 420.
[5] S. H. Strogatz, Phys. D **143**, 1 (2000).
[6] J. A. Acebrón, L. L. Bonilla, C. J. Pérez Vicente, F. Ritort, and R. Spigler, Rev. Mod. Phys. **77**, 137 (2005).
[7] F. A. Rodrigues, T. K. D. M. Peron, P. Ji, and J. Kurths, Phys. Rep. **610**, 1 (2016).
[8] I. Z. Kiss, Y. Zhai, and J. L. Hudson, Science **296**, 1676 (2002).
[9] M. K. S. Yeung and S. H. Strogatz, Phys. Rev. Lett. **82**, 648 (1999).
[10] W. S. Lee, E. Ott, and T. M. Antonsen, Phys. Rev. Lett. **103**, 044101 (2009).
[11] T. K. Dal'Maso Peron and F. A. Rodrigues, Phys. Rev. E **86**, 016102 (2012).
[12] L. L. Bonilla, J. C. Neu, and R. Spigler, J. Stat. Phys. **67**, 313 (1992).
[13] E. A. Martens, E. Barreto, S. H. Strogatz, E. Ott, P. So, and T. M. Antonsen, Phys. Rev. E **79**, 026204 (2009).
[14] D. Pazó and E. Montbrió, Phys. Rev. E **80**, 046215 (2009).
[15] J. Gõmez-Gardeñes, S. Gómez, A. Arenas, and Y. Moreno, Phys. Rev. Lett. **106**, 128701 (2011).
[16] I. Leyva, R. Sevilla-Escoboza, J. M. Buldú, I. Sendiña-Nadal, J. Gómez-Gardeñes, A. Arenas, Y. Moreno, S. Gõmez, R. Jaimes-Reátegui, and S. Boccaletti, Phys. Rev. Lett. **108**, 168702 (2012).
[17] P. Ji, T. K. D. M. Peron, P. J. Menck, F. A. Rodrigues, and J. Kurths, Phys. Rev. Lett. **110**, 218701 (2013).
[18] Y. Zou, T. Pereira, M. Small, Z. Liu, and J. Kurths, Phys. Rev. Lett. **112**, 114102 (2014).
[19] X. Hu, S. Boccaletti, W. Huang, X. Zhang, Z. Liu, S. Guan, and C.-H. Lai, Sci. Rep. **4**, 7262 (2014).
[20] X. Zhang, S. Boccaletti, S. Guan, and Z. Liu, Phys. Rev. Lett. **114**, 038701 (2015).
[21] S. Boccaletti, J. A. Almendral, S. Guan, I. Leyva, Z. Liu, I. Sendiña-Nadal, Z. Wang, and Y. Zou, Phys. Rep. **660**, 1 (2016).
[22] V. Nicosia, P. S. Skardal, A. Arenas, and V. Latora, Phys. Rev. Lett. **118**, 138302 (2017).
[23] J. Garcia-Ojalvo, M. B. Elowitz, and S. H. Strogatz, Proc. Natl. Acad. Sci. USA **101**, 10955 (2004).
[24] A. Kuznetsov, M. Kærn, and N. Kopell, SIAM J. Appl. Math. **65**, 392 (2004).
[25] E. Ullner, A. Zaikin, E. I. Volkov, and J. García-Ojalvo, Phys. Rev. Lett. **99**, 148103 (2007).
[26] T. Danino, O. Mondragón-Palomino, L. Tsimring, and J. Hasty, Nature (London) **463**, 326 (2010).
[27] A. F. Taylor, M. R. Tinsley, F. Wang, Z. Huang, and K. Showalter, Science **323**, 614 (2009).
[28] M. R. Tinsley, A. F. Taylor, Z. Huang, and K. Showalter, Phys. Rev. Lett. **102**, 158301 (2009).
[29] M. R. Tinsley, A. F. Taylor, Z. Huang, F. Wang, and K. Showalter, Phys. D **239**, 785 (2010).
[30] S. De Monte, F. d'Ovidio, S. Danø, and P. G. Sørensen, Proc. Natl. Acad. Sci. USA **104**, 18377 (2007).
[31] J. Zamora-Munt, C. Masoller, J. Garcia-Ojalvo, and R. Roy, Phys. Rev. Lett. **105**, 264101 (2010).
[32] W. Mather, J. Hasty, and L. S. Tsimring, Phys. Rev. Lett. **113**, 128102 (2014).
[33] D. J. Schwab, G. G. Plunk, and P. Mehta, Chaos **22**, 043139 (2012).
[34] D. J. Schwab, A. Baetica, and P. Mehta, Phys. D **241**, 1782 (2012).
[35] B. W. Li, C. B. Fu, H. Zhang, and X. G. Wang, Phys. Rev. E **86**, 046207 (2012).
[36] A. Sedra and P. Brackett, *Filter Theory and Design: Active and Passive* (Matrix, Beaverton, OR, 1978).
[37] T. L. Carroll, Phys. Rev. E **50**, 2580 (1994); IEEE Trans. Circ. Syst. I **42**, 105 (1995); Phys. Rev. E **53**, 3117 (1996).
[38] N. J. Corron and D. W. Hahs, IEEE Trans. Circ. Syst. I **44**, 373 (1997).
[39] R. Badii, G. Broggi, B. Derighetti, M. Ravani, S. Ciliberto, A. Politi, and M. A. Rubio, Phys. Rev. Lett. **60**, 979 (1988).
[40] P. Paoli, A. Politi, G. Broggi, M. Ravani, and R. Badii, Phys. Rev. Lett. **62**, 2429 (1989).
[41] F. Mitschke, Phys. Rev. A **41**, 1169 (1990).
[42] P. Blanchard and E. Brüning, *Mathematical Methods in Physics* (Birkhäuser, Boston, MA, 2003).
[43] E. Ott and T. M. Antonsen, Chaos **18**, 037113 (2008).
[44] E. Ott and T. M. Antonsen, Chaos **19**, 023117 (2009).
[45] All numerical integrations of the generalized Kuramoto model with LPF [Eqs. (3) and (4)] are performed by employing a standard explicit fourth-order Runge-Kutta method with an integration step of $h = 0.01$. In the simulations, two sets of numerical trials, termed *forward* and *backward* continuations [15], are adopted to monitor the stationary value of r as adiabatically increasing or decreasing K; i.e., the final states for the coupling strength K are used as the initial conditions for the next iteration of the coupling strength $K + \delta K$. In each calculation of r, the 100 000 transient iterations are discarded, and then the stationary value of r is obtained by averaging it over the next 100 000 iterations.